Science Advances
AAAS

Supplementary Materials for

Giant oscillatory Gilbert damping in superconductor/ferromagnet/ superconductor junctions

Yunyan Yao, Ranran Cai, Tao Yu, Yang Ma, Wenyu Xing, Yuan Ji, Xin-Cheng Xie, See-Hun Yang*, Wei Han*

*Corresponding author. Email: weihan@pku.edu.cn (W.H.); seeyang@us.ibm.com (S.-H.Y.)

Published 26 November 2021, *Sci. Adv.* **7**, eabh3686 (2021)
DOI: 10.1126/sciadv.abh3686

This PDF file includes:

Supplementary Materials and Methods

Section 1: Model of oscillating Gilbert damping above T_C.

The oscillatory Gilbert damping in normal metal (NM)/ferromagnet (FM)/NM heterostructures arising from quantum interference effect is analyzed based on previous theory by Mills (*36*). Within the linear response theory, the enhanced Gilbert damping is related to the dynamical spin susceptibility ($\chi^{-+}(\Omega)$) of conduction electrons in a FM,

$$\alpha_{\mathrm{sp}} = \frac{J^2 M_s V}{2N^2 \hbar^3 \gamma} \Lambda_2 \tag{S1}$$

where $\Lambda_2 = \mathrm{Im}\left(\frac{d\chi^{-+}(\Omega)}{d\Omega}\Big|_{\Omega=0}\right)$. Using one dimensional model, we obtain

$$\Lambda_2 = \frac{1}{\pi^2} \int_{\mathrm{FM}} dx dx' \mathrm{Im}[G_\uparrow(x, x', \epsilon_{\mathrm{F}})] \mathrm{Im}[G_\downarrow(x, x', \epsilon_{\mathrm{F}})] \tag{S2}$$

where $G_\sigma(x, x', \epsilon_{\mathrm{F}})$ is the Green's function for conduction electrons with σ-spin at the Fermi energy (ϵ_{F}). In a FM, $G_\sigma(x, x', \epsilon_{\mathrm{F}})$ is related to the exchange energy.

$$\left[-\frac{\hbar^2}{2m}\frac{d}{dx^2} - \epsilon \pm E_{\mathrm{ex}}\right] G_\sigma(x, x', \epsilon_{\mathrm{F}}) = \delta(x - x') \tag{S3}$$

For the FM film with a thickness d_{FM} in $-d_{\mathrm{FM}}/2 < x < d_{\mathrm{FM}}/2$, the Green's function satisfies the relation

$$G_\sigma(x, x', \epsilon_{\mathrm{F}}) = G_\sigma(x', x, \epsilon_{\mathrm{F}}) = G_\sigma(-x, -x', \epsilon_{\mathrm{F}}) \tag{S4}$$

Hence, the imaginary part of the Green's function could be expressed by

$$\mathrm{Im}[G_\sigma(x, x', \epsilon_{\mathrm{F}})] = -\pi\{N_{\mathrm{F}\sigma}\cos[k_{\mathrm{F}\sigma}(x-x')] + N'_{\mathrm{F}\sigma}\cos[k_{\mathrm{F}\sigma}(x+x')]\} \tag{S5}$$

where $k_{\mathrm{F}\sigma} = \sqrt{\frac{2m}{\hbar^2}(\epsilon_{\mathrm{F}} \mp E_{\mathrm{ex}})}$ is the Fermi wave-vector in the FM, $N_{\mathrm{F}\sigma}$ and $N'_{\mathrm{F}\sigma}$ are equivalent to the density of states and the modulation amplitude of the local density of states, respectively. For the same position of x, the local density of states is equal to

$$N_\sigma(x, \epsilon_{\mathrm{F}}) = N_{\mathrm{F}\sigma} + N'_{\mathrm{F}\sigma}\cos[2k_{\mathrm{F}\sigma}x] \tag{S6}$$

Since E_{ex} is much smaller compared to ϵ_{F}, the spatial modulation of the local density of states is negligible. The combination of equations (S2) and (S5) leads to

$$\Lambda_2 = \int_{-d_{\mathrm{FM}}/2}^{d_{\mathrm{FM}}/2} dx dx' \{N_{\mathrm{F}\uparrow}\cos[k_{\mathrm{F}\uparrow}(x-x')]\} * \{N_{\mathrm{F}\downarrow}\cos[k_{\mathrm{F}\downarrow}(x-x')]\} \tag{S7}$$

$$= 2N_{\mathrm{F}\uparrow}N_{\mathrm{F}\downarrow}\left\{\frac{1}{(k_{\mathrm{F}\uparrow}-k_{\mathrm{F}\downarrow})^2}\sin^2\left[\frac{k_{\mathrm{F}\uparrow}-k_{\mathrm{F}\downarrow}}{2}d_{\mathrm{FM}}\right]+\frac{1}{(k_{\mathrm{F}\uparrow}+k_{\mathrm{F}\downarrow})^2}\sin^2\left[\frac{k_{\mathrm{F}\uparrow}+k_{\mathrm{F}\downarrow}}{2}d_{\mathrm{FM}}\right]\right\}$$

Clearly, the enhanced Gilbert damping is expected to oscillate as a function of the FM thickness with two periods of $2\pi/[k_{\mathrm{F}\uparrow}-k_{\mathrm{F}\downarrow}]$ and $2\pi/[k_{\mathrm{F}\uparrow}+k_{\mathrm{F}\downarrow}]$. For real FM materials, such as NiFe with $(k_{\mathrm{F}\uparrow}+k_{\mathrm{F}\downarrow}) \gg (k_{\mathrm{F}\uparrow}-k_{\mathrm{F}\downarrow})$, the second term in the equation (S7) could be negligible, leaving only one oscillating period of $2\pi/[k_{\mathrm{F}\uparrow}-k_{\mathrm{F}\downarrow}]$. When the FM thickness is equal to $2n\pi/[k_{\mathrm{F}\uparrow}-k_{\mathrm{F}\downarrow}]$, a lower Gilbert damping is obtained. On the other hands with FM thickness of $(2n+1)\pi/[k_{\mathrm{F}\uparrow}-k_{\mathrm{F}\downarrow}]$, a larger Gilbert damping is obtained.

Section 2: Calculation of the enhanced Gilbert damping in Nb/NiFe/Nb by spin pumping via Andreev bound states (ABS).

As the reciprocal process of the spin transfer torque, conventional spin pumping is achieved by the magnetization torques provided by the driven quasiparticle carriers (*29, 52-54*), which are the electrons in the normal metals. In SC/FM heterostructures, however, the quasiparticle carriers can be either Bogoliubov quasiparticles or ABS (*42*), which lie above and within the superconducting gaps, respectively. Therefore, it is desirable to formulate and estimate the contribution to the spin pumping via the ABS (*26*), when the temperature is much smaller than the superconducting critical temperature.

Without loss of generality, we start the analysis from a left-propagating electron of energy ε and spin $\sigma = \{\uparrow, \downarrow\} = \{+, -,\}$. When the Zeeman splitting J is much smaller than the Fermi energy E_F, it has momentum

$$k_\sigma = k_F + (\varepsilon + \sigma J)/(\hbar v_F), \tag{S8}$$

where v_F is the Fermi velocity of the electron. When one electron goes from the FM to the SCs, it is reflected as a hole by the Andreev reflection at the right FM/SC interface; this hole has a phase shift $\chi = -\arccos(\varepsilon/\Delta)$ with respect to the electron (*55*), where Δ is the superconducting gap. Similarly, when a hole goes from the metal to the superconductor at the left FM/SC interface, an electron can be reflected. With a proper energy, the Andreev reflections can form a closed path, as a result of which the ABS forms. This requires that the phase accumulated in the reflections satisfies the Sommerfeld quantization condition, i.e. in the ballistic regime,

$$\frac{\varepsilon L}{\hbar v_F} + \sigma \frac{J d_{\mathrm{NiFe}}}{\hbar v_F} - \arccos\left(\frac{\varepsilon}{\Delta}\right) = n\pi + \frac{\varphi}{2}, \quad \text{(S9)}$$

where φ is the phase difference between the two superconductors, d_{NiFe} is the thickness of the FM layer and n is an integer. Since $\hbar v_F/\Delta \geq 100$ nm with $v_F = 2.2 \times 10^5$ m/s and $\Delta = 1$ meV at $T = 4$ K in our experiment (*17, 56, 57*), $d_{\mathrm{NiFe}} < 19$ nm $<< \hbar v_F/\Delta$ such that the first term in Eq. (S9) can be safely disregarded. For the FMR measurements with open-circuited configuration, the junctions always stay in the ground states (*43-45*). For π-junctions, there is a π-phase shift in the current-phase relationship curves compared to *zero*-junctions, i.e., the properties of $\varphi = 0$ of a π-junction is the same as those of $\varphi = \pi$ of a *zero*-junction. Since this π-phase shift is already taken into account by the FM exchange field, the ABS energy of the π-junctions can be obtained at $\varphi = 0$ in the ground states, which is similar to that of $\varphi = \pi$ of *zero*-junctions. Hence, the energy of the ABS can be described by $\varepsilon_0 = \pm\Delta\cos\left(\frac{J d_{\mathrm{NiFe}}}{\hbar v_F}\right)$ for ideal case with perfect transparency of electrons/holes.

In reality, the interfacial scattering and transport conditions (ballistic or diffusive regimes) of FM could affect the energy of the ABS. Following previous studies (*42, 58*), a transmission coefficient (D) could be introduced to describe this issue, which is close to unity in the ballistic regime but can also be large in the diffusive regime with an ideal transparency at the interface (*43, 59, 60*). In this work, we focus on the ideal cases with perfect transparency of electrons/holes. The energy of the ABS oscillates from the edge of the superconducting gap to the zero-energy with respect to the FM thickness (fig. S9A).

The pumped spin current reads (*29, 52-54*),

$$\mathbf{J}_s(t) = \frac{\hbar}{4\pi} g_{\mathrm{eff}}^{\uparrow\downarrow} \boldsymbol{m} \times \frac{d\boldsymbol{m}}{dt}, \quad \text{(S10)}$$

where $\boldsymbol{m}$ is the magnetization unit vector, and we define the effective mixing spin conductivity $g_{\mathrm{eff}}^{\uparrow\downarrow}$ at the finite temperature via the zero-temperature one $g^{\uparrow\downarrow}$ by (*26, 53*)

$$g_{\mathrm{eff}}^{\uparrow\downarrow} = n_0 \int d\varepsilon \frac{df(\varepsilon)}{d\varepsilon} \mathrm{Re}[g^{\uparrow\downarrow}(\varepsilon)]. \quad \text{(S11)}$$

Here, n_0 is the number of the conduction channel that roughly corresponds the conduction electron density at the interface and $f(\varepsilon) = 1/\{\exp[\varepsilon/(k_B T)] + 1\}$ is the Fermi-Dirac distribution of electron at the temperature T. Importantly, in the ballistic limit $\mathrm{Re}[g^{\uparrow\downarrow}(\varepsilon)] = 1$ when $\varepsilon = \varepsilon_0$; it

has width $\Delta\varepsilon$ depending on the FM thickness d_{NiFe} in the ballistic regime or the mean free path l_m in the diffusive regime. By the uncertainty principle, $\Delta\varepsilon\Delta t = 2\pi\hbar$, where $\Delta t = l_m/v_F$ is the propagation time of the electron in the junction, leading to $\Delta\varepsilon \sim 2\pi\hbar v_F/l_m$. By further considering the degeneracy due to spin (×2) and the existence of two interfaces (×2), we thus can estimate

$$g_{\mathrm{eff}}^{\uparrow\downarrow} \sim 8\pi n_0 \frac{\hbar v_F}{l_m} \frac{df(\varepsilon_0)}{d\varepsilon}. \tag{S12}$$

The pumped spin current carries the angular momentum away from the precessing magnetization and hence cause an enhanced Gilbert damping, which is described by

$$\delta\alpha = 2\gamma \frac{\hbar^2 v_F}{M_s l_m d_{\mathrm{NiFe}}} \frac{df(\varepsilon_0)}{d\varepsilon}, \tag{S13}$$

where γ is electron gyromagnetic ratio and M_s is the saturated magnetization of the ferromagnet.

We are now ready to estimate the contribution of ABS to the Gilbert damping at T = 4 K with varying transmission coefficient. We take n_0 =0.5 × 10^{16} m^{-2} following Ref. 44, l_m~ 3 nm, v_F= 2.2 × 10^5 m/s, J = 400 meV and $\mu_0 M_s \approx 1\,T$ from previous experimental results (*17*). With superconducting gaps $\Delta \approx 1$ meV at T = 4 K for Nb (*56, 57*), Fig. S8A plots the normalized energy of ABS by the superconducting gap at T = 4 K as a function of d_{NiFe} for the ideal transparency case. The oscillation of the Gilbert damping can be resolved by using the FM exchange field-induced phase shift of $\frac{Jd_{\mathrm{NiFe}}}{\hbar v_F}$ (fig. S9B). For simplicity, we have disregarded the possible thickness dependence of the superconducting gaps and magnetizations. To be noted, our theoretical estimation is based on a simplified model that assumes D = 1. For the diffusive regime or the case of non-perfect transparency of electrons at the interface (*42, 43*), similar oscillating behaviors of ABS (or DOS) in the SCs can also be preserved. For example, the oscillating ABS (or DOS) in the SCs have been shown to exist in the diffusive regime theoretically (*6, 46*), and indeed, the *zero* to π transitions have been experimentally observed in both the ballistic and diffusive regimes from the supercurrent measurements (*11, 17*). To fully understand the experimental observation of the oscillatory Gilbert damping in the diffusive regime, further theoretical studies are needed.

Section 3: Measurement of the Josephson coupling in Nb/NiFe/Nb.

The Nb/NiFe/Nb Josephson devices are fabricated using the shadow mask techniques during the films growth. As shown in figs. S7A and S7B, the Josephson devices have a junction area (A) of ~ 80 μm × 80 μm, and the other areas are electrically isolated by a 100 nm AlO_x layer. The Josephson current is measured by standard a.c. lock-in technique. The normalized differential resistances (dV/dI) measured on the Nb/NiFe (5 nm)/Nb junction at various temperatures are shown in fig. S7C. The critical current (I_c) is defined as point where the differential resistance increases above the value for the zero-bias current. The normal resistance (R_n) is determined to be the saturated value of the normal states of the Josephson coupling measurement. The measured area-resistance product (R_nA) of ~ $5 \times 10^{-10}\ \Omega m^2$ is higher than that reported in metallic Josephson junction (*17, 61*), and comparable to that of FM Josephson junction with a thin tunnel barrier (*62*). This behavior indicates that there is more likely a thin $NiFeO_x$ layer (indicated by Fig. S8B) in the junction formed during the AlO_x growth step in the presence of oxygen gas. As the temperature increases, I_c and the characteristic voltage (I_cR_n) decrease (figs. S7C and S7D). Clear Josephson currents are observed on the Nb/NiFe (5 nm)/Nb junction and Nb/NiFe (10 nm)/Nb junction (figs. S7E and S78F). And the estimated SC gap energy is ~ 0.9 meV at T = 2 K (*1, 43*), which is comparable to the value of ~1.36 meV at T = 0 K estimated from T_C of ~ 8.5 K (fig. S4). On the other hand, no Josephson current could be observed in the Nb/NiFe (30 nm)/Nb junction (figs. S7E and S7F). The absence of Josephson current in Nb/NiFe (30 nm)/Nb junction indicates that there is no long-range spin-triplet Josephson coupling in the Nb/NiFe/Nb heterostructures in our experiment.

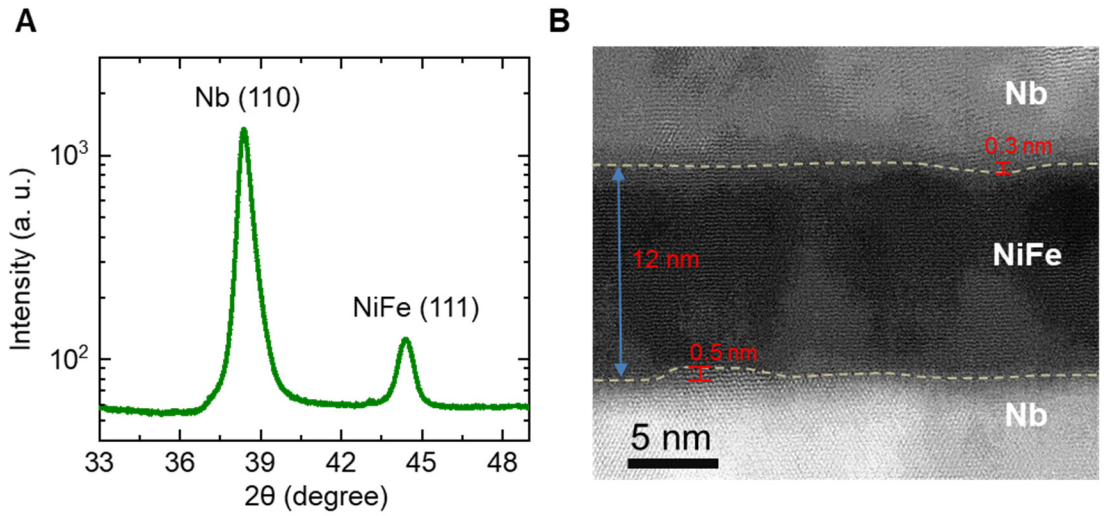

fig. S1. The crystalline properties of the Nb/NiFe/Nb heterostructures. (**A**) The θ-2θ X-ray diffraction results measured on the typical Nb/NiFe (12 nm)/Nb sample, where Nb (110) and NiFe (111) peaks are observed. (**B**) High-resolution transmission electron micrographs measured on the typical Nb/NiFe (12 nm)/Nb sample. The dashed lines show the interfaces between Nb and NiFe layers. The red bars indicate the deviation of NiFe at the interface.

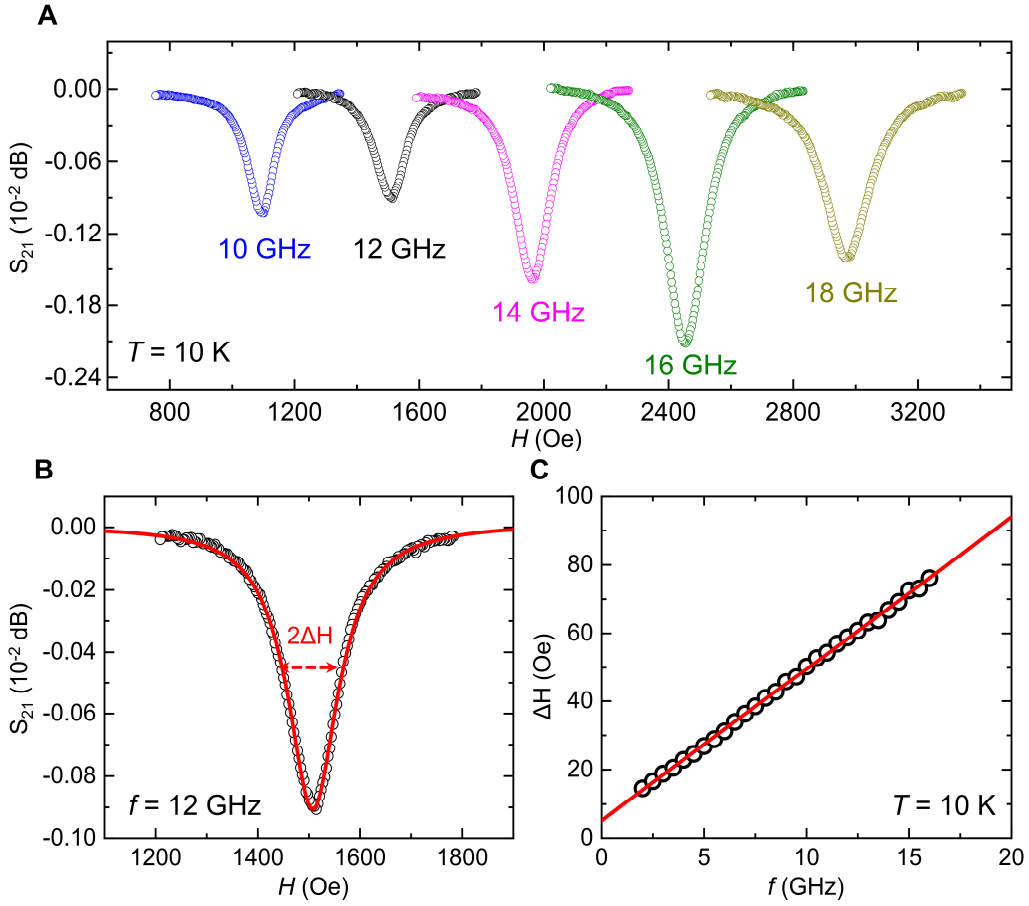

fig. S2. Gilbert damping measurement of Nb/NiFe/Nb heterostructures at T = 10 K. (**A**) The typical FMR spectra as a function of magnetic field with microwave frequency (f) of 10, 12, 14, 16, and 18 GHz, respectively. (**B**) The typical FMR spectrum measured with f = 12 GHz (black circles) and the Lorentz fitting curve (red line). ΔH is the half linewidth of the FMR signal. (**C**) The determination of the Gilbert damping from ΔH vs. f. The red line indicates the best linear-fitting curve. These results are obtained on the typical Nb/Py (12 nm)/Nb sample.

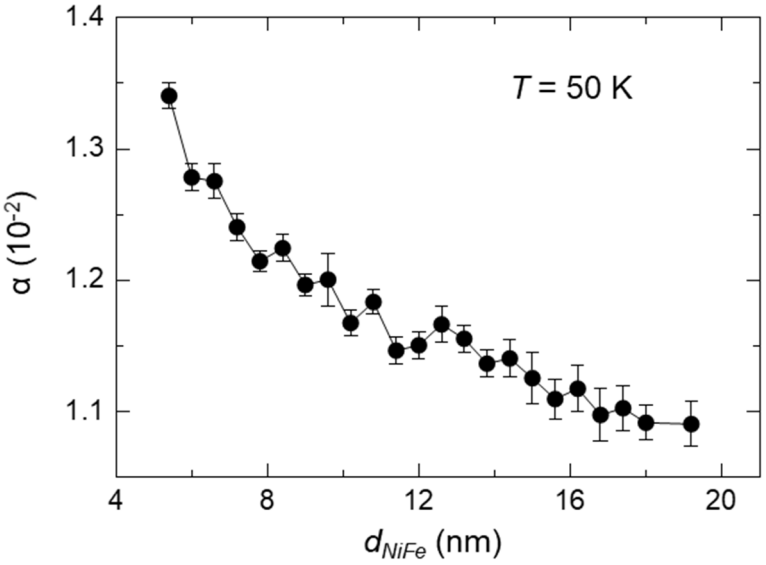

fig. S3. NiFe thickness dependence of Gilbert damping at T = 50 K.

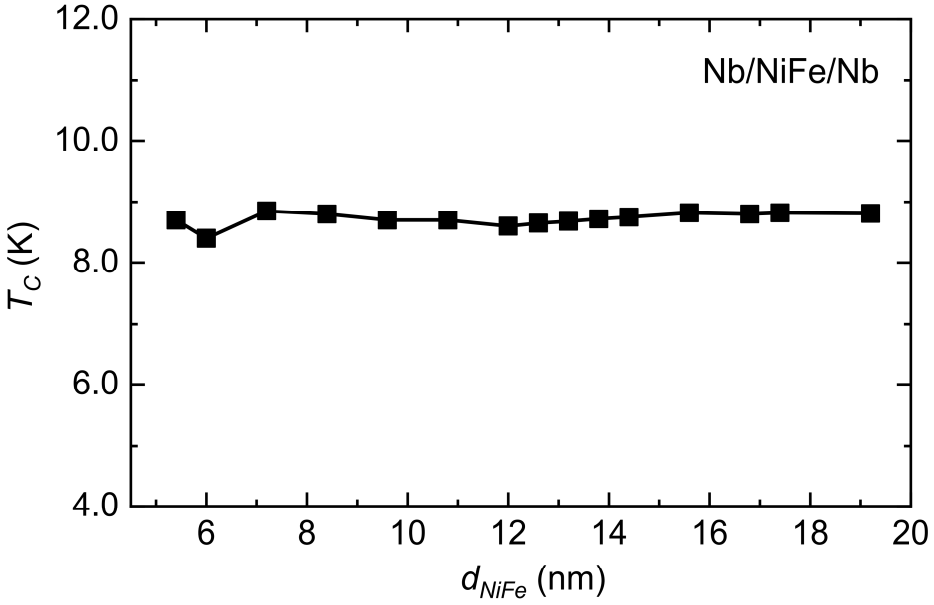

fig. S4. NiFe thickness dependence of T_C for the Nb/NiFe/Nb heterostructures. The T_C is determined from the zero-resistance temperature via four-probe resistance measurement.

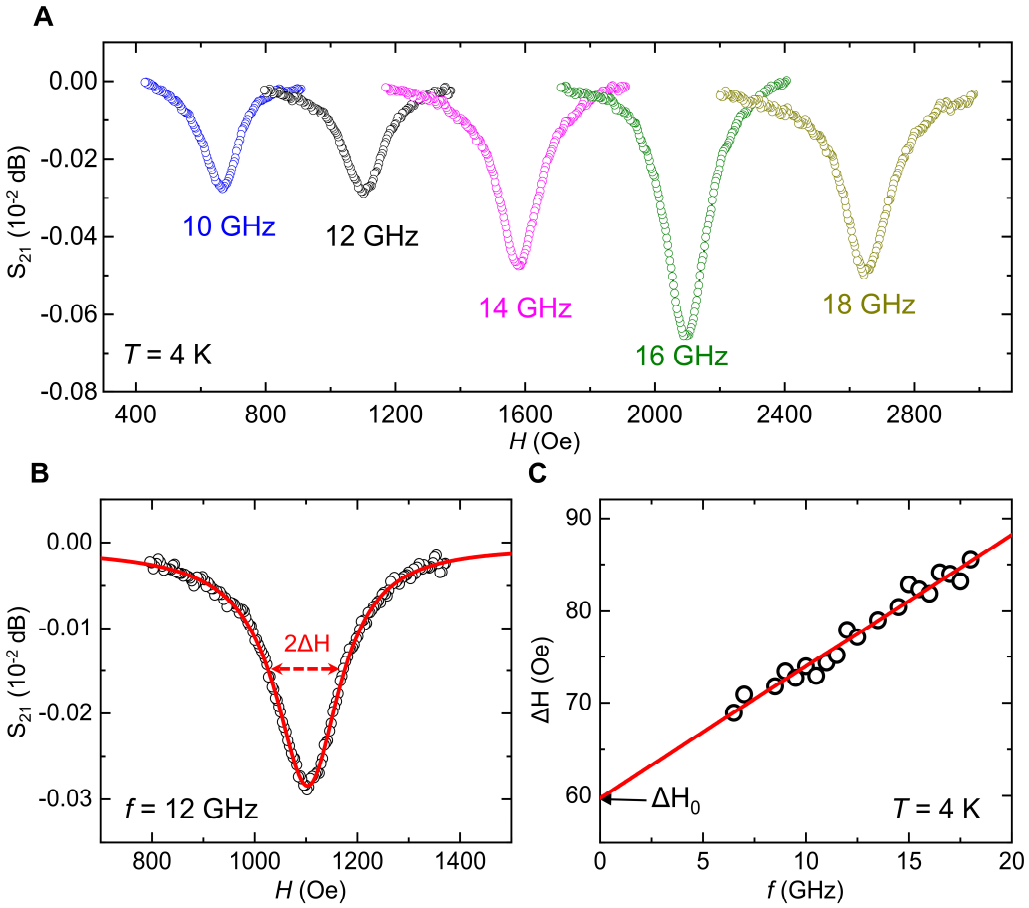

fig. S5. Measurement of the Gilbert damping of Nb/NiFe/Nb heterostructures at $T = 4$ K. (**A**) The typical FMR spectra as a function of magnetic field with microwave frequency (f) of 10, 12, 14, 16, and 18 GHz, respectively. (**B**) The typical FMR spectrum measured with $f = 12$ GHz (black circles) and the Lorentz fitting curve (red line). ΔH is the half linewidth of the FMR signal. (**C**) The determination of the Gilbert damping from ΔH vs. f. The red line indicates the best linear-fitting curve. These results are obtained on the typical Nb/Py (12 nm)/Nb sample.

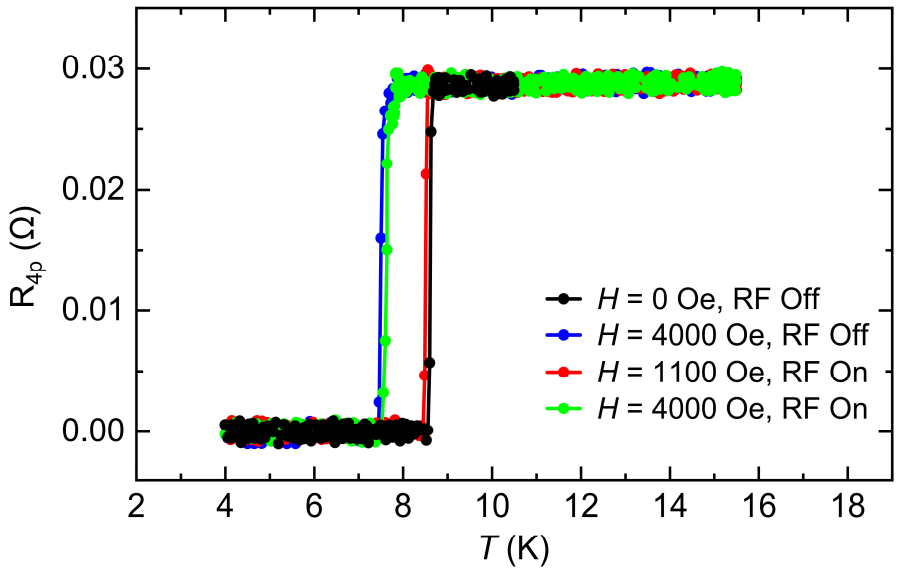

fig. S6. The effect of FMR measurement on the T_C of Nb/NiFe/Nb heterostructures. The four-probe resistances *vs.* temperature are probed from the typical Nb/NiFe (12 nm)/Nb sample with/without the presence of the in-plane magnetic field and microwave power.

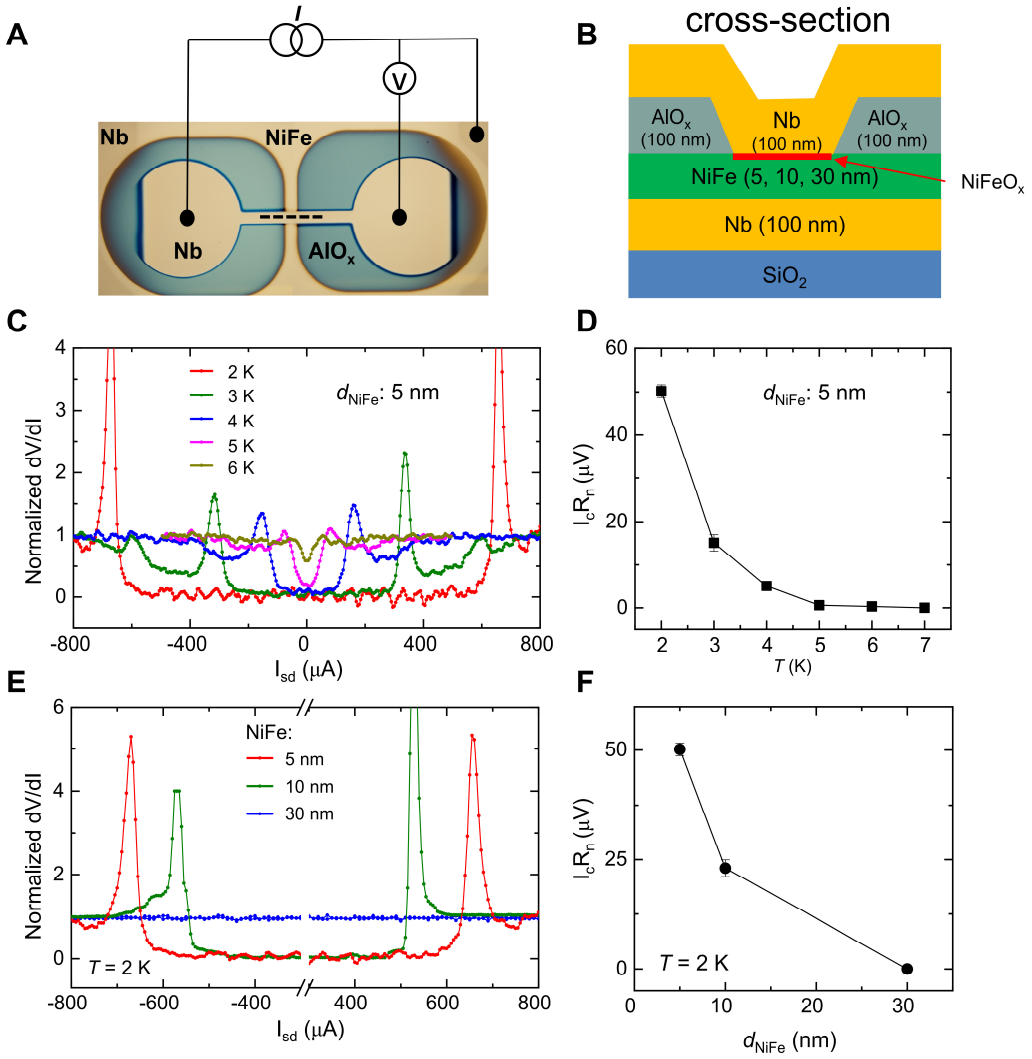

fig. S7. The measurement of Josephson coupling in Nb/NiFe/Nb junctions. (**A**) The optical image of a typical Nb/NiFe/Nb Josephson device and schematic of the electrical measurement geometry. (**B**) The cross-section of the Josephson devices with a junction area of ~ 80 μm × 80 μm. At the junction, a thin oxide layer of $NiFeO_x$ is mostly liked formed on the top surface of NiFe during the growth of AlO_x in the presence of oxygen. (**C**) The normalized differential resistance (dV/dI) as a function of the bias current measured on the Nb/NiFe (5 nm)/Nb junction from $T = 2$ to 6 K. (**D**) The temperature dependence of the characteristic voltage (I_cR_n) of the Nb/NiFe (5 nm)/Nb Josephson junction. (**E**) The normalized differential resistance as a function of the bias current of the Nb/NiFe/Nb junctions (d_{NiFe} = 5, 10 and 30 nm) at $T = 2$ K. (**F**) The NiFe thickness dependence of the characteristic voltages at $T = 2$ K.

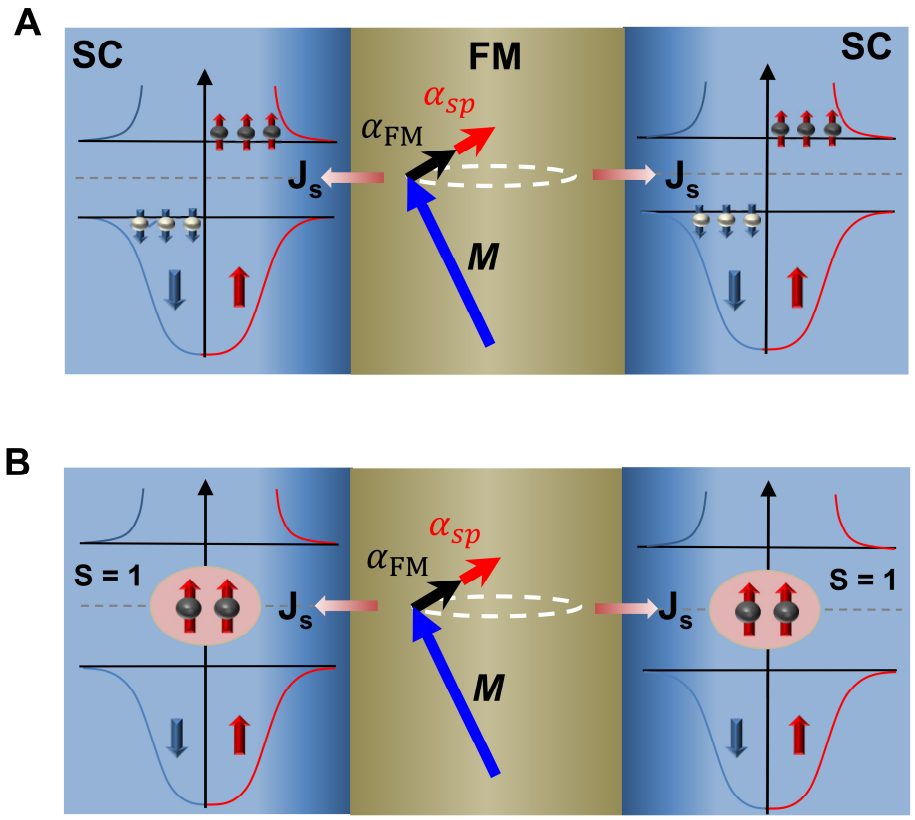

fig. S8. Illustration of magnetization dynamics and spin pumping in the SC/FM/SC heterostructures due to Bogoliubov quasiparticles (A) and equal spin-triplet Cooper pairs (B). The dark and light balls represent the electron-like and hole-like quasiparticles respectively. The red and blue arrows indicate the spin up and spin down respectively.

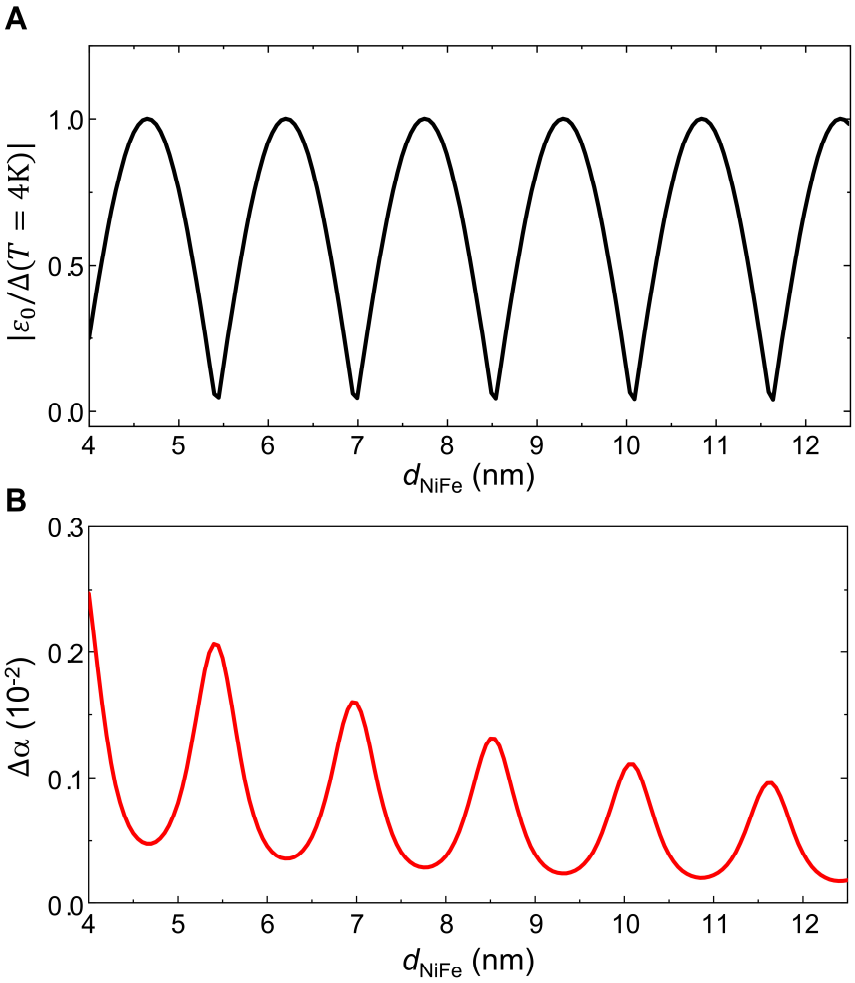

fig. S9. Calculation of the enhanced Gilbert damping due to spin pumping via the ABS at T = 4 K. (**A**) The normalized energy of ABS by the superconducting gap at $T = 4$ K as a function of d_{NiFe} for the ideal transparency case. (**B**) The enhanced Gilbert damping via ABS as a function of d_{NiFe}.

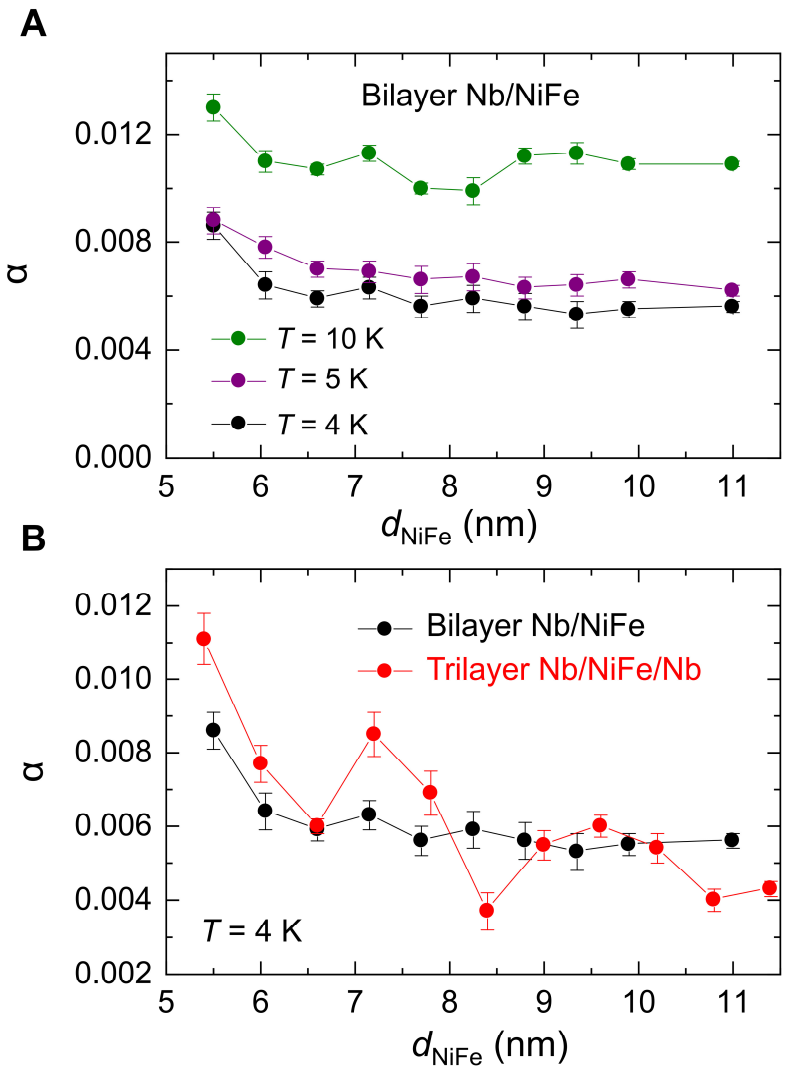

fig. S10. Gilbert damping of control sample of bilayer Nb/NiFe junctions. (A) Gilbert damping of bilayer Nb/NiFe junctions at T = 4, 5, and 10 K. **(B)** Comparison of the Gilbert damping of bilayer Nb/NiFe and trilayer Nb/NiFe/Nb junctions at T = 4 K.

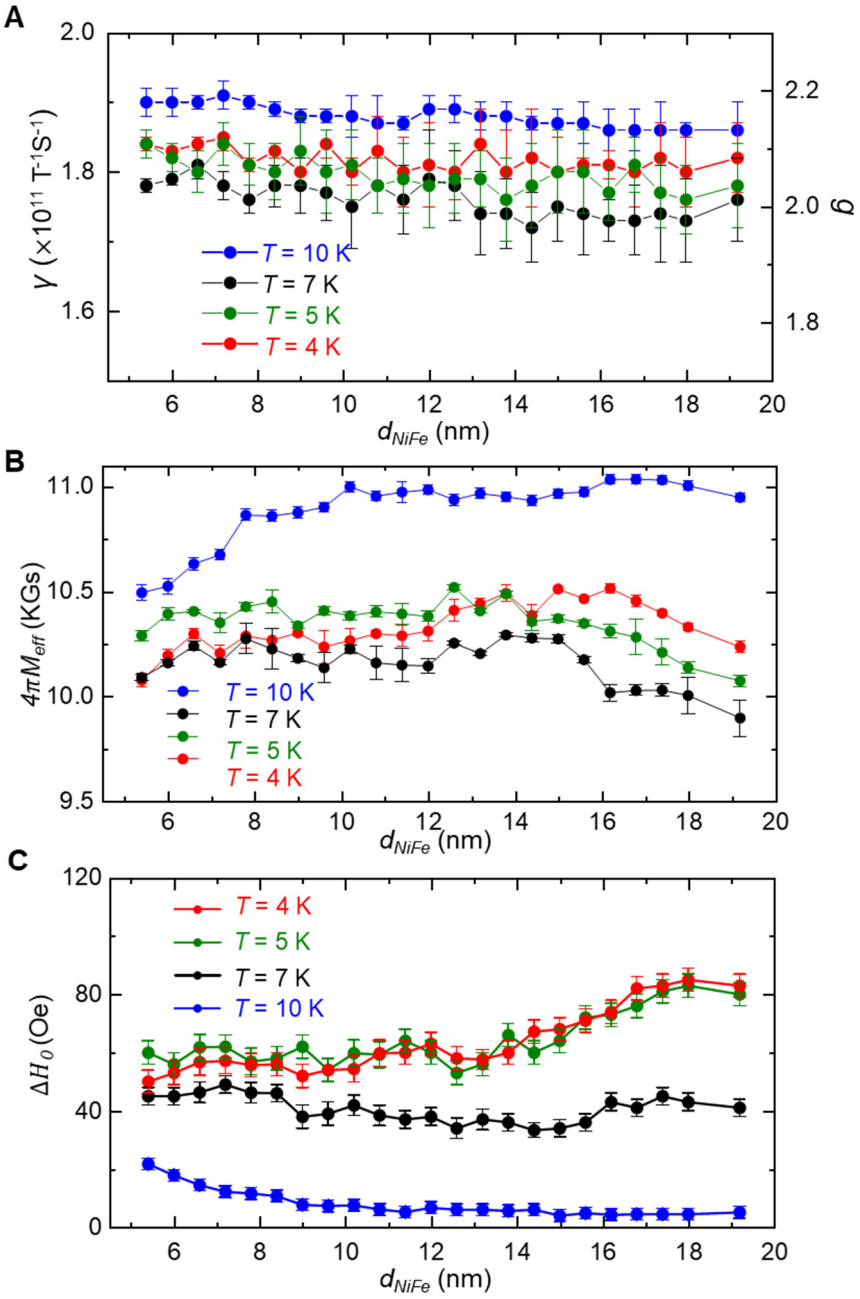

fig. S11. Thickness dependence of gyromagnetic ratio (and g factor) (A), effective magnetization (B) and inhomogeneous half-linewidth (C). The blue, black, green and red dotted-lines represent to temperature of T = 10, 7, 5 and 4 K, respectively.

REFERENCES AND NOTES

1. A. I. Buzdin, Proximity effects in superconductor-ferromagnet heterostructures. *Rev. Mod. Phys.* **77**, 935–976 (2005).

2. F. S. Bergeret, A. F. Volkov, K. B. Efetov, Odd triplet superconductivity and related phenomena in superconductor-ferromagnet structures. *Rev. Mod. Phys.* **77**, 1321–1373 (2005)..

3. J. Linder, J. W. A. Robinson, Superconducting spintronics. *Nat. Phys.* **11**, 307–315 (2015).

4. M. Eschrig, J. Kopu, J. C. Cuevas, G. Schön, Theory of half-metal/superconductor heterostructures. *Phys. Rev. Lett.* **90**, 137003 (2003).

5. A. I. Buzdin, L. N. Bulaevskii, S. V. Panyukov, Critical-current oscillations as a function of the exchange field and thickness of the ferromagnetic metal (F) in an SFS Josephson junction. *JETP Lett.* **35**, 178–180 (1982).

6. T. Kontos, M. Aprili, J. Lesueur, X. Grison, Inhomogeneous superconductivity induced in a ferromagnet by proximity effect. *Phys. Rev. Lett.* **86**, 304–307 (2001).

7. L. B. Ioffe, V. B. Geshkenbein, M. V. Feigel'man, A. L. Fauchère, G. Blatter, Environmentally decoupled sds -wave Josephson junctions for quantum computing. *Nature* **398**, 679–681 (1999).

8. J. E. Mooij, T. P. Orlando, L. Levitov, L. Tian, C. H. van der Wal, S. Lloyd, Josephson persistent-current qubit. *Science* **285**, 1036–1039 (1999).

9. T. Yamashita, K. Tanikawa, S. Takahashi, S. Maekawa, Superconducting π qubit with a ferromagnetic Josephson junction. *Phys. Rev. Lett.* **95**, 097001 (2005).

10. T. Kontos, M. Aprili, J. Lesueur, F. Genêt, B. Stephanidis, R. Boursier, Josephson junction through a thin ferromagnetic layer: Negative coupling. *Phys. Rev. Lett.* **89**, 137007 (2002).

11. J. W. A. Robinson, S. Piano, G. Burnell, C. Bell, M. G. Blamire, Critical current oscillations in strong ferromagnetic π junctions. *Phys. Rev. Lett.* **97**, 177003 (2006).

12. M. Weides, M. Kemmler, H. Kohlstedt, R. Waser, D. Koelle, R. Kleiner, E. Goldobin, 0−π Josephson tunnel junctions with ferromagnetic barrier. *Phys. Rev. Lett.* **97**, 247001 (2006).

13. C. Bell, R. Loloee, G. Burnell, M. G. Blamire, Characteristics of strong ferromagnetic Josephson junctions with epitaxial barriers. *Phys. Rev. B* **71**, 180501 (2005).

14. V. V. Ryazanov, V. A. Oboznov, A. Y. Rusanov, A. V. Veretennikov, A. A. Golubov, J. Aarts, Coupling of two superconductors through a ferromagnet: Evidence for a π junction. *Phys. Rev. Lett.* **86**, 2427–2430 (2001).

15. Y. Blum, A. Tsukernik, M. Karpovski, A. Palevski, Oscillations of the superconducting critical current in Nb-Cu-Ni-Cu-Nb junctions. *Phys. Rev. Lett.* **89**, 187004 (2002).

16. V. Shelukhin, A. Tsukernik, M. Karpovski, Y. Blum, K. B. Efetov, A. F. Volkov, T. Champel, M. Eschrig, T. Löfwander, G. Schön, A. Palevski, Observation of periodic π-phase shifts in ferromagnet-superconductor multilayers. *Phys. Rev. B* **73**, 174506 (2006).

17. J. W. A. Robinson, S. Piano, G. Burnell, C. Bell, M. G. Blamire, Zero to π transition in superconductor-ferromagnet-superconductor junctions. *Phys. Rev. B* **76**, 094522 (2007).

18. C. Bell, S. Milikisyants, M. Huber, J. Aarts, Spin dynamics in a superconductor-ferromagnet proximity system. *Phys. Rev. Lett.* **100**, 047002 (2008).

19. Y. Yao, Q. Song, Y. Takamura, J. P. Cascales, W. Yuan, Y. Ma, Y. Yun, X. C. Xie, J. S. Moodera, W. Han, Probe of spin dynamics in superconducting NbN thin films via spin pumping. *Phys. Rev. B* **97**, 224414 (2018).

20. K.-R. Jeon, C. Ciccarelli, A. J. Ferguson, H. Kurebayashi, L. F. Cohen, X. Montiel, M. Eschrig, J. W. A. Robinson, M. G. Blamire, Enhanced spin pumping into superconductors provides evidence for superconducting pure spin currents. *Nat. Mater.* **17**, 499–503 (2018).

21. M. Müller, L. Liensberger, L. Flacke, H. Huebl, A. Kamra, W. Belzig, R. Gross, M. Weiler, M. Althammer, Temperature-dependent spin transport and current-induced torques in superconductor-ferromagnet heterostructures. *Phys. Rev. Lett.* **126**, 087201 (2021).

22. J. P. Morten, A. Brataas, G. E. W. Bauer, W. Belzig, Y. Tserkovnyak, Proximity-effect–assisted decay of spin currents in superconductors. *Europhys. Lett.* **84**, 57008 (2008).

23. M. Inoue, M. Ichioka, H. Adachi, Spin pumping into superconductors: A new probe of spin dynamics in a superconducting thin film. *Phys. Rev. B* **96**, 024414 (2017).

24. T. Kato, Y. Ohnuma, M. Matsuo, J. Rech, T. Jonckheere, T. Martin, Microscopic theory of spin transport at the interface between a superconductor and a ferromagnetic insulator. *Phys. Rev. B* **99**, 144411 (2019).

25. M. A. Silaev, Large enhancement of spin pumping due to the surface bound states in normal metal--superconductor structures. *Phys. Rev. B* **102**, 180502 (2020).

26. M. T. Ahari, Y. Tserkovnyak, Superconductivity-enhanced spin pumping: Role of Andreev resonances. *Phys. Rev. B* **103**, L100406 (2021).

27. W. Han, S. Maekawa, X.-C. Xie, Spin current as a probe of quantum materials. *Nat. Mater.* **19**, 139–152 (2020).

28. R. H. Silsbee, A. Janossy, P. Monod, Coupling between ferromagnetic and conduction-spin-resonance modes at a ferromagnetic\normal-metal interface. *Phys. Rev. B* **19**, 4382–4399 (1979).

29. Y. Tserkovnyak, A. Brataas, G. E. W. Bauer, B. I. Halperin, Nonlocal magnetization dynamics in ferromagnetic heterostructures. *Rev. Mod. Phys.* **77**, 1375–1421 (2005).

30. L. Landau, E. Lifshitz, On the theory of the dispersion of magnetic permeability in ferromagnetic bodies. *Phys. Z. Sowjetunion* **8**, 153 (1935).

31. T. L. Gilbert, A phenomenological theory of damping in ferromagnetic materials. *IEEE Trans. Magn.* **40**, 3443–3449 (2004).

32. J. C. Slonczewski, Current-driven excitation of magnetic multilayers. *J. Magn. Magn. Mater.* **159**, L1-L7 (1996).

33. J. A. Sauls, Andreev bound states and their signatures. *Philos. Trans. Royal Soc. A* **376**, 20180140 (2018).

34. M. Eschrig, Theory of Andreev bound states in S-F-S junctions and S-F proximity devices. *Phil. Trans. R. Soc. A* **376**, 20150149 (2018).

35. S. S. P. Parkin, N. More, K. P. Roche, Oscillations in exchange coupling and magnetoresistance in metallic superlattice structures: Co/Ru, Co/Cr, and Fe/Cr. *Phys. Rev. Lett.* **64**, 2304–2307 (1990).

36. D. L. Mills, Ferromagnetic resonance relaxation in ultrathin metal films: The role of the conduction electrons. *Phys. Rev. B* **68**, 014419 (2003).

37. T. Wakamura, H. Akaike, Y. Omori, Y. Niimi, S. Takahashi, A. Fujimaki, S. Maekawa, Y. Otani, Quasiparticle-mediated spin Hall effect in a superconductor. *Nat. Mater.* **14**, 675–678 (2015).

38. C. Holmqvist, S. Teber, M. Fogelström, Nonequilibrium effects in a Josephson junction coupled to a precessing spin. *Phys. Rev. B* **83**, 104521 (2011).

39. M. Tinkham, *Introduction to Superconductivity* (Dover Publications, 2004).

40. M. Eschrig, T. Löfwander, Triplet supercurrents in clean and disordered half-metallic ferromagnets. *Nat. Phys.* **4**, 138–143 (2008).

41. M. Houzet, Ferromagnetic Josephson junction with precessing magnetization. *Phys. Rev. Lett.* **101**, 057009 (2008).

42. C. W. J. Beenakker, Universal limit of critical-current fluctuations in mesoscopic Josephson junctions. *Phys. Rev. Lett.* **67**, 3836–3839 (1991).

43. A. A. Golubov, M. Y. Kupriyanov, E. Il'ichev, The current-phase relation in Josephson junctions. *Rev. Mod. Phys.* **76**, 411–469 (2004).

44. H. Sellier, C. Baraduc, F. Lefloch, R. Calemczuk, Half-integer Shapiro steps at the 0-π crossover of a ferromagnetic Josephson junction. *Phys. Rev. Lett.* **92**, 257005 (2004).

45. E. Strambini, A. Iorio, O. Durante, R. Citro, C. Sanz-Fernández, C. Guarcello, I. V. Tokatly, A. Braggio, M. Rocci, N. Ligato, V. Zannier, L. Sorba, F. S. Bergeret, F. Giazotto, A Josephson phase battery. *Nat. Nanotechnol.* **15**, 656–660 (2020).

46. M. Zareyan, W. Belzig, Y. V. Nazarov, Oscillations of Andreev states in clean ferromagnetic films. *Phys. Rev. Lett.* **86**, 308–311 (2001).

47. T. Wakamura, N. Hasegawa, K. Ohnishi, Y. Niimi, Y. Otani, Spin injection into a superconductor with strong spin-orbit coupling. *Phys. Rev. Lett.* **112**, 036602 (2014).

48. C. Chappert, K. L. Dang, P. Beauvillain, H. Hurdequint, D. Renard, Ferromagnetic resonance studies of very thin cobalt films on a gold substrate. *Phys. Rev. B* **34**, 3192–3197 (1986).

49. W. Platow, A. N. Anisimov, G. L. Dunifer, M. Farle, K. Baberschke, Correlations between ferromagnetic-resonance linewidths and sample quality in the study of metallic ultrathin films. *Phys. Rev. B* **58**, 5611–5621 (1998).

50. Y. Zhao, Q. Song, S.-H. Yang, T. Su, W. Yuan, S. S. P. Parkin, J. Shi, W. Han, Experimental investigation of temperature-dependent Gilbert damping in permalloy thin films. *Sci. Rep.* **6**, 22890 (2016).

51. K.-R. Jeon, C. Ciccarelli, H. Kurebayashi, L. F. Cohen, X. Montiel, M. Eschrig, T. Wagner, S. Komori, A. Srivastava, J. W. A. Robinson, M. G. Blamire, Effect of Meissner screening and trapped magnetic flux on magnetization dynamics in thick Nb/$Ni_{80}Fe_{20}$/Nb trilayers. *Phys. Rev. Appl.* **11**, 014061 (2019).

52. Y. Tserkovnyak, A. Brataas, G. E. W. Bauer, Enhanced Gilbert damping in thin ferromagnetic films. *Phys. Rev. Lett.* **88**, 117601 (2002).

53. H. J. Skadsem, A. Brataas, J. Martinek, Y. Tserkovnyak, Ferromagnetic resonance and voltage-induced transport in normal metal-ferromagnet-superconductor trilayers. *Phys. Rev. B* **84**, 104420 (2011).

54. T. Yu, G. E. W. Bauer, Noncontact spin pumping by microwave evanescent fields. *Phys. Rev. Lett.* **124**, 236801 (2020).

55. A. F. Andreev, The thermal conductivity of the intermediate state in superconductors. *JETP* **19**, 1228 (1964).

56. P. Townsend, J. Sutton, Investigation by electron tunneling of the superconducting energy gaps in Nb, Ta, Sn, and Pb. *Phys. Rev.* **128**, 591–595 (1962).

57. A. V. Pronin, M. Dressel, A. Pimenov, A. Loidl, I. V. Roshchin, L. H. Greene, Direct observation of the superconducting energy gap developing in the conductivity spectra of niobium. *Phys. Rev. B* **57**, 14416–14421 (1998).

58. D. G. C. Jones, Quantum transport. Introduction to nanoscience, by Y.V. Nazarov and Y.M. Blanter. *Contemp. Phys.* **51**, 379–380 (2010).

59. Y. V. Nazarov, Limits of universality in disordered conductors. *Phys. Rev. Lett.* **73**, 134–137 (1994).

60. T. T. Heikkilä, J. Särkkä, F. K. Wilhelm, Supercurrent-carrying density of states in diffusive mesoscopic Josephson weak links. *Phys. Rev. B* **66**, 184513 (2002).

61. J. Bass, W. P. Pratt Jr., Spin-diffusion lengths in metals and alloys, and spin-flipping at metal/metal interfaces: An experimentalist's critical review. *J. Phys. Condens. Matter* **19**, 183201 (2007).

62. A. A. Bannykh, J. Pfeiffer, V. S. Stolyarov, I. E. Batov, V. V. Ryazanov, M. Weides, Josephson tunnel junctions with a strong ferromagnetic interlayer. *Phys. Rev. B* **79**, 054501 (2009).